Statistical analysis of injection/dispersion events in Saturn's inner magnetosphere

Y. Chen[1] and T. W. Hill[1]

Received 18 March 2008; revised 5 May 2008; accepted 15 May 2008; published 26 July 2008.

[1] In the inner magnetosphere of a rapidly rotating planet such as Jupiter and Saturn, radial transport of plasma mainly comprises hot, tenuous plasma moving inward and cold, denser plasma moving outward. A distinctive phenomenon resulting from the drift dispersion of injecting hot plasma provides direct evidence for this convective motion. Particle instruments aboard the Cassini spacecraft, including the Magnetospheric Imaging Instrument (MIMI) and the Cassini Plasma Spectrometer (CAPS), have made numerous observations of such signatures. The statistics of the properties of such events are studied in this paper by analyzing CAPS data from 26 Cassini orbits. A statistical picture of their major characteristics is developed, including the distributions of ages, longitudinal widths, radial distances, and longitudes and local times of injection. An unexpected longitude modulation of these events appears in the old SLS longitude system, which is based on the Saturn kilometric radiation (SKR) observations by Voyager around 1980, while no such modulation seems to exist in the new SKR longitude system of the Cassini era. A Lomb periodogram analysis, however, reveals no significant periodic modulation of these events. The injection structures are found to occupy a small fraction ($\sim$5–10) of the available longitude space.

Citation: Chen, Y., and T. W. Hill (2008), Statistical analysis of injection/dispersion events in Saturn's inner magnetosphere, *J. Geophys. Res.*, *113*, A07215, doi:10.1029/2008JA013166.

1. Introduction

[2] In a rotation-dominated magnetosphere with internal plasma sources, radial transport of plasma is expected to be triggered by the centrifugal interchange instability [*Hill*, 1976; *Siscoe and Summers*, 1981], in which cold flux tubes with larger densities move outward and exchange locations with hotter, more tenuous flux tubes. The process of this radial convection has been studied by numerous theoretical models [e.g., *Hill et al.*, 1981; *Pontius et al.*, 1986] and numerical simulations [*Yang et al.*, 1994; *Wu et al.*, 2007a, 2007b], and was confirmed by observations in Jupiter's magnetosphere [*Mauk et al.*, 1997, 1999].

[3] While moving in the radial direction, electrons and ions with different energies become dispersed in the longitudinal direction and hence arrive at the spacecraft at different times. Observational signatures of this process are referred to as injection/dispersion events and have been observed frequently by the Cassini Plasma Spectrometer (CAPS) [*Young et al.*, 2005] and the Cassini Magnetospheric Imaging Instrument (MIMI) [*Krimigis et al.*, 2005] since Cassini's first orbit at Saturn in July 2004. Several previous studies [e.g., *Burch et al.*, 2005; *Hill et al.*, 2005; *Mauk et al.*, 2005] have interpreted these events as evidence for interchange instability in Saturn's magnetosphere.

[4] Figure 1, reproduced from *Hill et al.* [2005], shows a localized injection of hot plasma accompanied by adiabatic gradient and curvature drifts. It is expected that while particles are injected by $E \times B$ drift in the radial direction, gradient-curvature drifts in the longitudinal direction will separate electrons from ions, forming a V-shaped structure in a linear energy versus longitude spectrogram. Because these structures are swept past the spacecraft by the fast rotational flow, they can be directly observed on a linear energy versus time spectrogram [*Hill et al.*, 2005, Figure 2]. Straight lines were fit to each leg of the "V" in order to analyze the properties of each event, with ions forming the left halves and electrons forming the right halves. In Saturn's corotating frame, gradient and curvature drifts move electrons westward and ions eastward. Therefore, in an energy-time spectrogram, high-energy ions are expected to be observed first, followed in sequence by lower-energy ions, lower-energy electrons, and finally high-energy electrons.

[5] As the injection/dispersion process develops with time, the distance between ions and electrons grows. The age of the injection is inversely proportional to the slope of each leg of the V structure. For standard gradient/curvature drifts in Saturn's dipole magnetic field, the relationship is

$$\frac{dE}{dt} = \left(-6.87\frac{keV}{\min}\right)\left(\frac{10}{L}\right)\left(\frac{1hr}{T_{inj}}\right)\left(\frac{\Omega}{\Omega_s}\right)sign(q) \qquad (1)$$

Here L denotes the dipole L value (equatorial distance in units of Saturn's radius R_s = 60,300 km), Ω_s represents

[1]Department of Physics and Astronomy, Rice University, Houston, Texas, USA.

0148-0227/08/2008JA013166$09.00

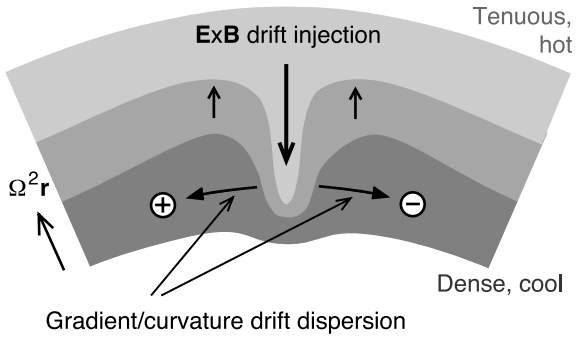

Figure 1. Conceptual illustration of an injection-dispersion event, reproduced from Figure 1 of *Hill et al.* [2005].

Saturn's rotation frequency, Ω is the angular velocity at which an injection/dispersion structure is swept past the spacecraft by the rotational flow, T_{inj} is the time since injection, and q is the particle charge. Strictly speaking, this equation assumes the injection/dispersion process takes place in the equatorial plane. Our study only covers a very limited latitude range, so it is adequate to use this equation. Moreover, equation (1) strictly applies only for particles mirroring in the equatorial plane, but it is adequate for particles of any pitch angle within a factor of order unity.

[6] Other properties of these events can also be estimated from observation. For example, the longitudinal width can be obtained by multiplying the width in time δt by the partial corotation velocity, i.e.,

$$Width = LR_s\Omega\delta t \tag{2}$$

The local time of injection is related to the local time of observation by

$$LT_{inj} = LT_{obs} - \Omega T_{inj} \tag{3}$$

Finally, the injection longitude can be calculated from

$$\lambda_{inj} = \lambda_{obs} - (\Omega - \Omega_s)T_{inj} \tag{4}$$

[7] *Hill et al.* [2005] reported about 100 such events observed by CAPS during Cassini's first two orbits of Saturn, with a subset of 48 selected for study. Their work included a statistical analysis, which indicated that the ages of the injection/dispersion events ranged from several hours to several Saturn rotation periods, and longitudinal widths ranged from less than one Saturn radius to several radii. In

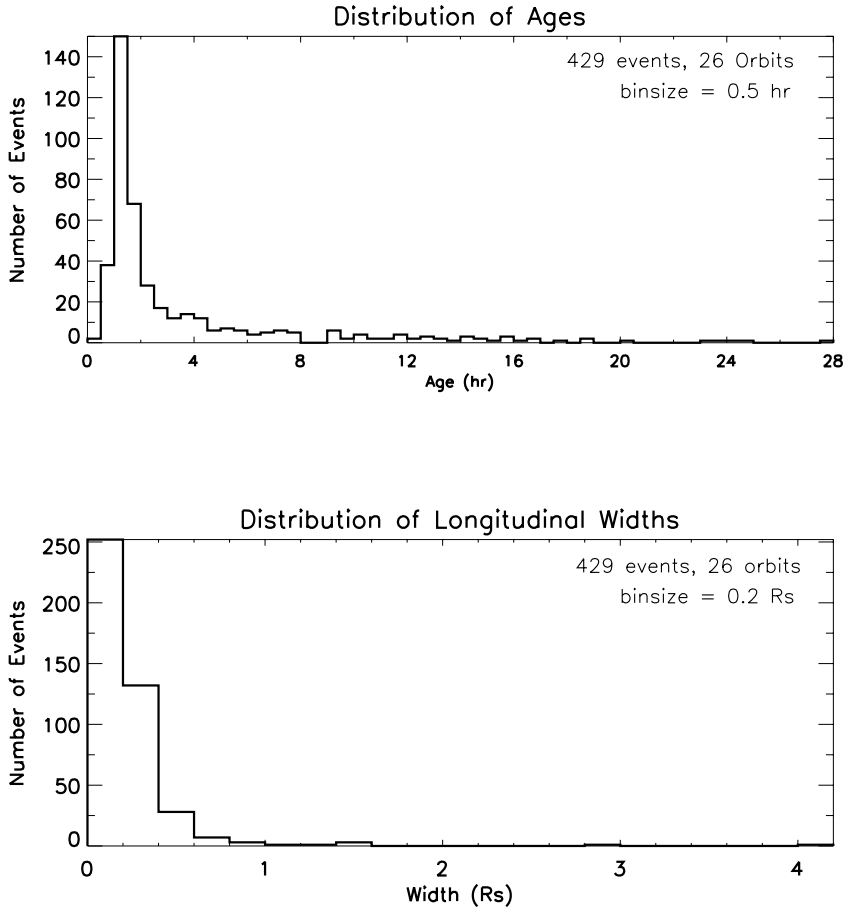

Figure 2. Statistical distributions of (top) the ages and (bottom) the longitudinal widths of 429 injection-dispersion events selected from 26 orbits of Cassini Plasma Spectrometer data.

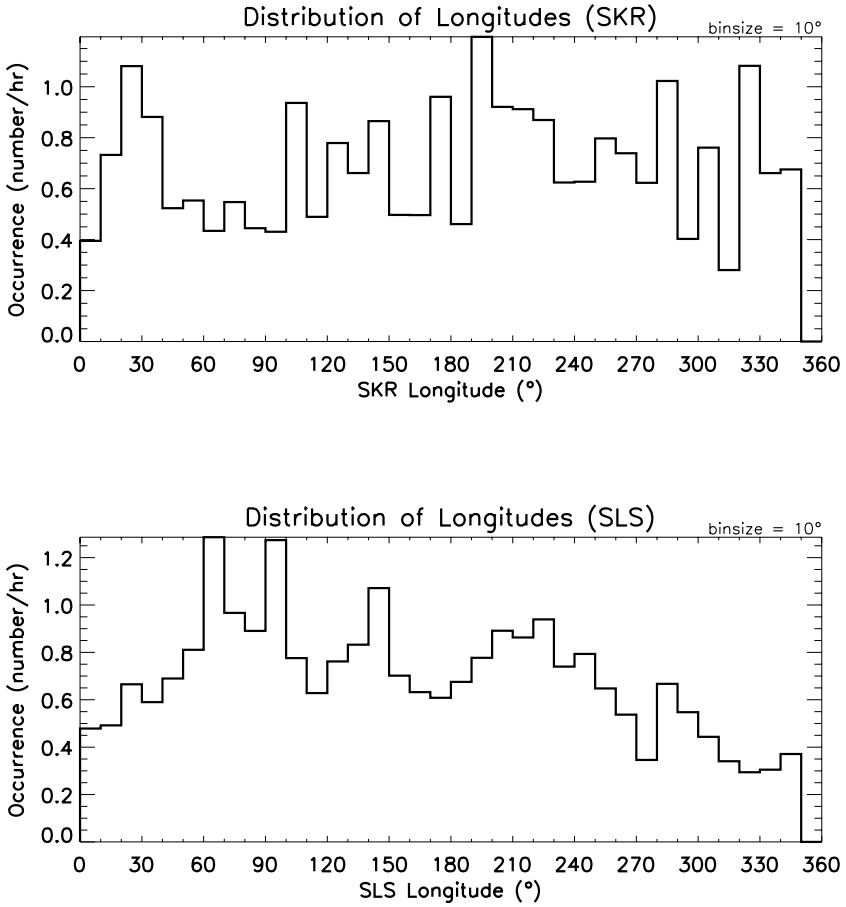

Figure 3. Statistical distributions of the injection longitudes for two different systems, (top) SKR and (bottom) SLS. Only those 410 events located inside the radial distance range [5,10] are included. Here the vertical axes represent the occurrence frequencies instead of number of events.

addition, most of the events were located in the radial range $5 < L < 10$, while the local time distribution and longitude distribution were both random in appearance. The assumption of rigid corotation was made ($\Omega = \Omega_s$) because at that time there was not enough analysis of the ion velocity moments to provide azimuthal velocities. This assumption was probably an overestimate of rotational velocity; as a result, ages, widths, and injection longitudes were overestimated, while injection local times were underestimated.

2. Analysis of Properties

[8] We continue the statistical analysis of the properties of the injection/dispersion events, and extend it to a larger sample space. With many more orbits of observation since Cassini's Saturn Orbit Insertion (SOI), we are now able to include a much larger data set in our study, extending from June 2004 to the end of August 2006. Similar methods to those of *Hill et al.* [2005] are used to estimate the characteristics of the injection/dispersion structures.

[9] In addition to expanding the statistical data set, we are also able now to utilize observed rotational velocities as reported recently by *Wilson et al.* [2007]. The following second-order polynomial fit to the measurements of Wilson et al. is used to specify Ω(L) in equations (1), (2), (3), and (4).

$$V_\varphi = 79.56 - 13.06R + 1.30R^2 \quad (5)$$

Here V_φ is the rotational velocity in km/s and R is the radial distance in R_S. This is an improvement over the rigid corotation assumption, although we still have to assume that the azimuthal velocity is the same at all longitudes on a given L shell.

[10] As before, the analysis procedure still depends on subjective judgment, which inevitably introduces errors when reading the observable properties from the spectrograms. To limit the impacts of this error source, we adopt a set of selection criteria to limit our analysis to the most unambiguous events. Specifically, each event we selected here has an identifiable center time, i.e., the intersection of the structure legs with the time axis; the width of the legs must also be identifiable; and the slopes of the legs must be reliably measurable. With these criteria, we selected 429 structures for analysis, located between the radial distances 4.6 and 14.8 Saturn radii. Of these 429 events, 410 clustered between L values of 5 and 10, i.e., more than 95% of the total.

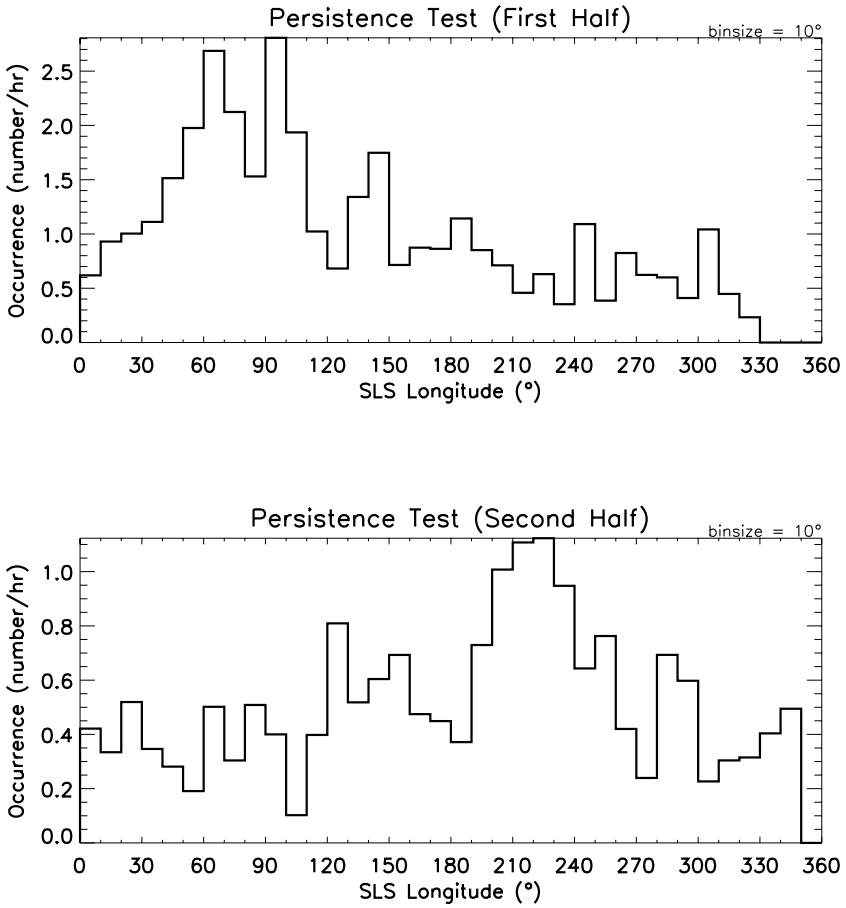

Figure 4. Persistence test of the longitudinal modulation in the SLS system, displaying the distributions of the injection longitudes (SLS) for the (top) first and (bottom) second halves by time, respectively. Only the 410 events located inside the radial distance range [5,10] are included.

[11] The results reported below are based on the CAPS Electron Spectrometer (ELS) electron data only. Many of the structures do not have clear ion components because ion count rates are much lower than electron count rates in a given plasma environment.

3. Statistical Results

[12] Here we use histograms to display statistical distributions of various properties of injection/dispersion events. Figure 2 (top) shows the age distribution of all 429 events, while Figure 2 (bottom) shows the distribution of longitudinal widths. One can conclude that most of the events have ages of less than 2 h and widths of less than one Saturn radius. However, some events are as old as several Saturn rotation periods and as wide as several Saturn radii. These results are consistent with those of *Hill et al.* [2005]. Note that the lower limits on both the ages and the widths are among the selection criteria, so that very young events, as discussed by *Burch et al.* [2005], might not be identified here. The lower limit for ages is about 0.25 h, while the lower limit for widths is about 0.1 Saturn radii. Upper limits on ages and widths are also implied by the selection criteria, which tend to rule out both very old structures and very large-scale ones.

[13] One thing that we are interested in is the distribution of injection longitudes, from which we can obtain information about the modulation of these events by Saturn's rotating magnetosphere. A recently defined longitude system, the Saturn Kilometric Radiation (SKR) system [*Kurth et al.*, 2007], is now widely used. It is a dynamic system with a variable period that follows the rotational modulation. Several magnetospheric phenomena have been reported to be well organized by this system, including SKR itself by definition [*Kurth et al.*, 2007], magnetic field perturbations [*Giampieri et al.*, 2006], electron density in the inner magnetosphere [*Gurnett et al.*, 2007], and the energetic particle flux in the outer magnetosphere [*Carbary et al.*, 2007a]. An immediate question hence arises: could the injection/dispersion events also be modulated by this SKR longitude system? Our analysis is motivated in part to address this question, using data obtained in the time range from January 2004 to August 2006, when the SKR system was accurately applicable [*Kurth et al.*, 2008].

[14] In Figure 3, the upper panel shows the distribution of occurrence frequencies of the injection/dispersion events versus their injection longitude in the SKR system. To obtain the occurrence frequency in a given longitude bin, we divide the number of events found in that bin by the time Cassini spent in the same sector. From the histogram, we conclude that the occurrence of injection/dispersion events

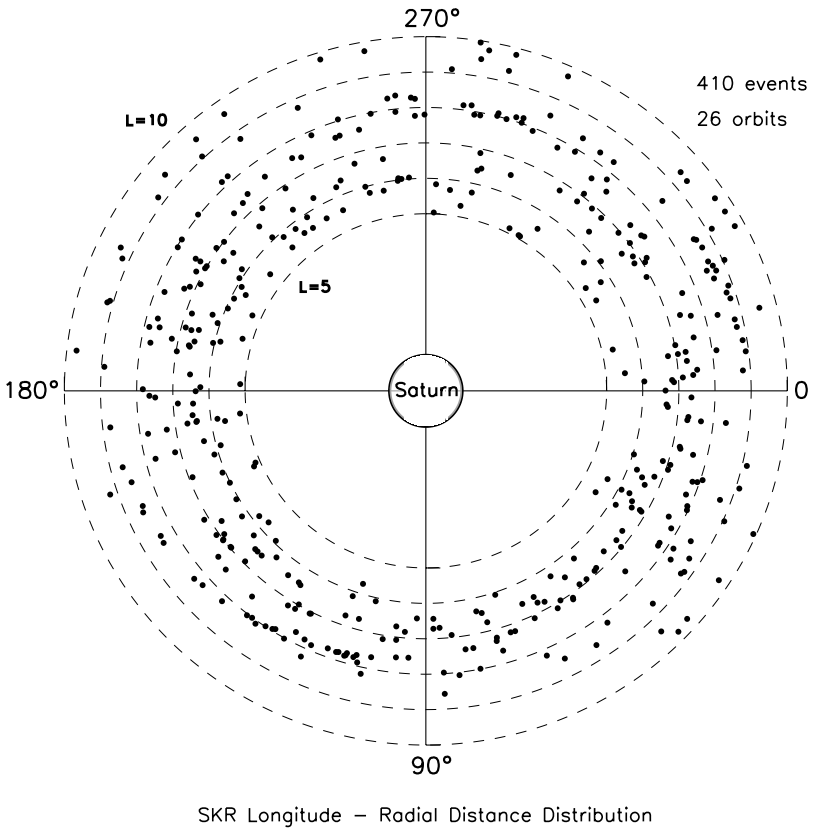

Figure 5. Statistical distributions of the injection longitudes (SKR) in the polar coordinate system. Only the 410 events located inside the radial distance range [5,10] are included.

is randomly distributed with regard to injection longitude in the SKR system, as there is no obvious clustering at any particular longitude.

[15] Interestingly, a different picture (Figure 3, bottom) emerges when we use the Saturn Longitude System (SLS) [*Seidelmann et al.*, 2002] instead of the SKR system. SLS was adopted by the International Astronomical Union (IAU) based on Voyager-era observations of the period of SKR. The injection/dispersion events seem to be organized surprisingly well by SLS longitude, in that the occurrence frequency is systematically larger in the longitude range $\sim$50–250° than outside this range.

[16] The SLS longitude modulation is surprising when we consider that most other magnetospheric phenomena have

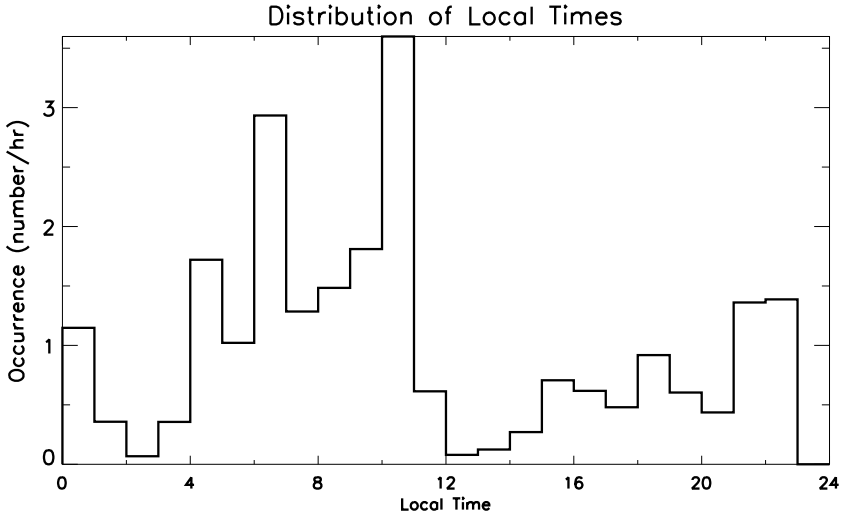

Figure 6. Statistical distributions of the injection local times. Only the 410 events located inside the radial distance range [5,10] are included. Here the vertical axes represent the occurrence frequencies instead of number of events.

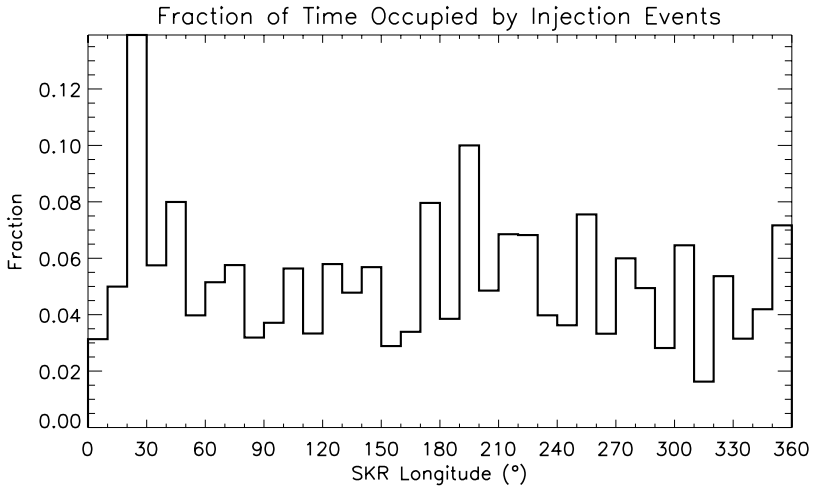

Figure 7. Fraction of time occupied by injection events versus SKR longitude.

been found to be modulated by the SKR system. Could this modulation in the SLS system be a sporadic or transient effect? A persistence test is designed to check the persistence of the data in time. We simply separate the data set into two halves by time and plot the histogram of occurrence frequencies for each half. The results are shown in Figure 4, where the first half of the data is plotted in Figure 4 (top) and the second half in Figure 4 (bottom). There is an apparent modulation in both halves but also a "phase shift" between the first half and the second half. This phase shift suggests that the modulation period, if any, is not SLS exactly, but slower by about one part in 2000. (By comparison, the SKR rate is about 1% slower than the SLS rate.)

[17] In addition to the rotational modulation of magnetospheric phenomena, a spiral pattern has been identified by *Espinosa et al.* [2003], *Cowley et al.* [2006], and *Gurnett et al.* [2007] in magnetic field perturbations, and by *Carbary et al.* [2007b] in high-energy electron fluxes (28–48 keV) in the SKR longitude system, at radial distances larger than 10 Saturn radii. To investigate whether there is a similar modulation pattern in the injection/dispersion events, we plot these events in the equatorial plane of the polar SKR coordinate system (Figure 5), showing both their radial and longitudinal locations. Note that the longitude coordinate is a left-handed angle. No spiral pattern is apparent, although we cannot rule out the possibility of multiple short-lived spirals having different phases.

[18] To show the local-time distribution of injections, we plotted a histogram of occurrence frequency versus different local time bins (Figure 6). There is an apparent local-time asymmetry, with a clustering of plasma injections in the pre-noon quadrant. This is certainly not the local-time distribution that one would expect from an Earth-like convection system in which virtually all injections occur on the nightside.

[19] Finally, the fraction of the time that is occupied by injection events is calculated for 10° longitude bins. To obtain this fraction for a given longitude sector, we sum over the widths in time of all the events observed in that sector, i.e., the width of one leg of each "V" structure, and divide this by the total time that the spacecraft spent in the same longitude sector in the radial range $5 < L < 10$. The results are shown in Figure 7, where one can see that most values of this fraction are less than 0.1, with a mean value of about 0.05. This gives a sense of the fraction of the available longitude space that is occupied by inflow regions,

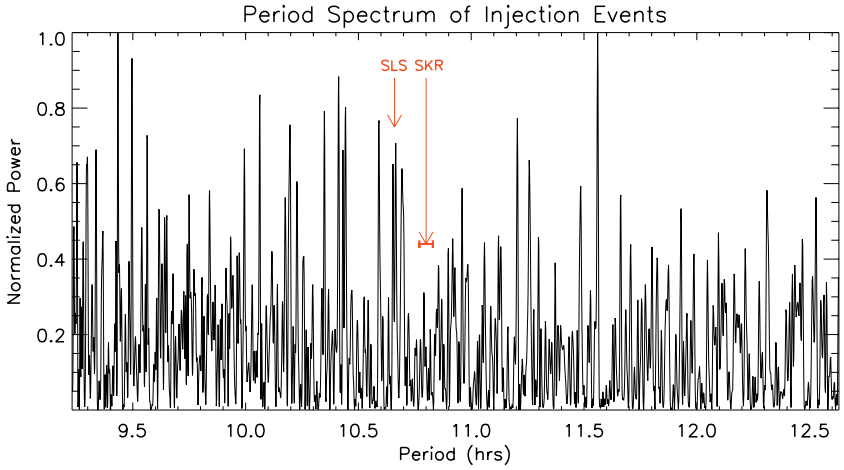

Figure 8. Lomb periodogram for all the selected events. Data have been detrended and smoothed.

which is a useful constraint for numerical simulation of the process [e.g., *Wu et al.*, 2007b].

4. Periodogram Analysis

[20] To further study the possible periodicity of these events, we have done a periodogram analysis, for which we converted our data to a time series. A simple step function was adopted to obtain a time series, with the values set to one inside an injection structure, and zero elsewhere. If there are several injections going on at the same time, we add one to the function's value for each event.

[21] After the time series is obtained, the major problem for a periodicity analysis is the fact that our time series is unevenly spaced. As stated above, we are focusing on the inner part of Saturn's magnetosphere, since most of the events are found when the Cassini spacecraft was in the range $5 < L < 10$. Our data set has huge gaps when the spacecraft is not in this range. Hence, the commonly used spectrum techniques such as the Fast Fourier Transform (FFT) are impractical because the Fourier Transform only works with series that are evenly spaced in time. Instead, we have applied the so-called Lomb-Scargle Algorithm (or the ''Lomb periodogram''), which also returns a power spectrum like the FFT, but is designed to handle unevenly spaced data. The Lomb periodogram can test the hypothesis that the time series contains a significant periodic signal by returning a ''significance number'' with values ranging in the interval [0, 1.0]. The smaller this number is, the more significant the periodic signal is. This algorithm was applied to determine the periods of some other magnetospheric phenomena and has returned favorable outcomes for the magnetic field [*Giampieri et al.*, 2006] and the energetic particles [*Carbary et al.*, 2007a].

[22] There is an existing procedure in the Interactive Data Language (IDL) library which is based on the routine *fasper* from *Press et al.* [1992], named LNP_TEST. After a smoothing and detrending process, this procedure was applied directly. Figure 8 shows the normalized power spectrum, where the frequency axis has been converted to time in order to represent the period directly. The most significant feature of this result is its lack of features; instead, a forest of peaks fills the interval between 9.5 h and 12.5 h, with no particularly significant peaks that might represent a dominant period in the original data.

5. Conclusions

[23] Through the analysis of CAPS electron data, we have compiled statistics of over 400 injection/dispersion events observed during 2 years of Cassini measurements. The results reported here on the ages and longitude widths are consistent with the previous study [*Hill et al.*, 2005], showing that the injection/dispersion events are mesoscale structures which typically last several hours. These events are not organized well by the Cassini-era SKR longitude system. Instead, they display a possible modulation at the Voyager-era SLS period, although a periodogram analysis reveals no significant periodicity. The local time distribution reveals a curious asymmetry in which the events tend to cluster in the prenoon quadrant.

[24] A significant result of our study is that injections occupy a small fraction, ~5–10%, of the available longitudinal space. This result quantifies the general impression that Saturn's rotation-driven convection system comprises narrow sectors of rapid inflow surrounded by broader regions of slower outflow.

[25] Many injection events have very small ages, as discussed by *Burch et al.* [2005]. These very young events were excluded by the selection criteria in our present study. Additional work is needed to include these young events in our data set.

[26] **Acknowledgments.** We have benefited from discussions with Alex Dessler, Krishan Khurana, and Vytenis Vasyliunas. This work was supported by NASA JPL contract 1243218 to the Southwest Research Institute.

[27] Wolfgang Baumjohann thanks Abigail Rymer and another reviewer for their assistance in evaluating this paper.

References

Burch, J. L., J. Goldstein, T. W. Hill, D. T. Young, F. J. Crary, A. J. Coates, N. Andre, W. S. Kurth, and E. C. Sittler Jr. (2005), Properties of local plasma injections in Saturn's magnetosphere, *Geophys. Res. Lett.*, *32*, L14S02, doi:10.1029/2005GL022611.

Carbary, J. F., D. G. Mitchell, S. M. Krimigis, D. C. Hamilton, and N. Krupp (2007a), Charged particle periodicities in Saturn's outer magnetosphere, *J. Geophys. Res.*, *112*, A06246, doi:10.1029/2007JA012351.

Carbary, J. F., D. G. Mitchell, S. M. Krimigis, and N. Krupp (2007b), Evidence for spiral pattern in Saturn's magnetosphere using the new SKR longitudes, *Geophys. Res. Lett.*, *34*, L13105, doi:10.1029/2007GL030167.

Cowley, S. W. H., D. M. Wright, E. J. Bunce, A. C. Carter, M. K. Dougherty, G. Giampieri, J. D. Nichols, and T. R. Robinson (2006), Cassini observations of planetary-period magnetic field oscillations in Saturn's magnetosphere: Doppler shifts and phase motion, *Geophys. Res. Lett.*, *33*, L07104, doi:10.1029/2005GL025522.

Espinosa, S. A., D. J. Southwood, and M. K. Dougherty (2003), How can Saturn impose its rotation period in a noncorotating magnetosphere?, *J. Geophys. Res.*, *108*(A2), 1086, doi:10.1029/2001JA005084.

Giampieri, G., M. K. Dougherty, E. J. Smith, and C. T. Russell (2006), A regular period for Saturn's magnetic field that may track its internal rotation, *Nature*, *441*, 62–64, doi:10.1038/nature04750.

Gurnett, D. A., A. M. Persoon, W. S. Kurth, J. B. Groene, T. F. Averkamp, M. K. Dougherty, and D. J. Southwood (2007), The variable rotation period of the inner region of Saturn's plasma disk, *Science*, doi:10.1126/science.1138562.

Hill, T. W. (1976), Interchange stability of a rapid rotating magnetosphere, *Planet. Space Sci.*, *24*, 1151–1154, doi:10.1016/0032-0633(76)90152-5.

Hill, T. W., et al. (1981), Corotating magnetospheric convection, *J. Geophys. Res.*, *86*, 9020–9028, doi:10.1029/JA086iA11p09020.

Hill, T. W., A. M. Rymer, J. L. Burch, E. J. Crary, D. T. Young, M. F. Thomsen, D. Delapp, N. Andre, A. J. Coates, and G. R. Lewis (2005), Evidence for rotationally driven plasma transport in Saturn's magnetosphere, *Geophys. Res. Lett.*, *32*, L14S10, doi:10.1029/2005GL022620.

Krimigis, S. M., et al. (2005), Dynamics of Saturn's magnetosphere from MIMI during Cassini's orbital insertion, *Science*, *307*, 1270–1273, doi:10.1126/science.1105978.

Kurth, W. S., A. Lecacheux, T. F. Averkamp, J. B. Groene, and D. A. Gurnett (2007), A Saturnian longitude system based on a variable kilometric radiation period, *Geophys. Res. Lett.*, *34*, L02201, doi:10.1029/2006GL028336.

Kurth, W. S., T. F. Averkamp, D. A. Gurnett, J. B. Groene, and A. Lecacheux (2008), An update to a Saturn longitude system based on kilometric radio emissions, *J. Geophys. Res.*, *113*, A05222, doi:10.1029/2007JA012861.

Mauk, B. H., D. J. Williams, and R. W. McEntire (1997), Energy-time dispersed charged particle signatures of dynamic injections in Jupiter's inner magnetosphere, *Geophys. Res. Lett.*, *24*, 2949–2952, doi:10.1029/97GL03026.

Mauk, B. H., et al. (1999), Storm-like dynamics of Jupiter's inner magnetosphere, *J. Geophys. Res.*, *104*, 22,759–22,778, doi:10.1029/1999JA900097.

Mauk, B. H., et al. (2005), Energetic particle injections in Saturn's magnetosphere, *Geophys. Res. Lett.*, *32*, L14S05, doi:10.1029/2005GL022485.

Pontius, D. H., Jr., T. W. Hill, and M. E. Rassbach (1986), Steady state plasma transport in a corotation-dominated magnetosphere, *Geophys. Res. Lett.*, *13*, 1097–1100, doi:10.1029/GL013i011p01097.

Press, W. H., S. A. Teukolsky, W. T. Vetterling, and B. P. Flannery (1992), *Numerical Recipes: The Art of Scientific Computing*, pp. 569–577, Cambridge Univ. Press, Cambridge, U. K.

Seidelmann, P. K., et al. (2002), Report of the IUA/IAG working group on cartographic coordinates and rotational elements of the planets and satellites:2000, *Celestial Mech. Dyn. Astron.*, *82*, 83–110, doi:10.1023/A:1013939327465.

Siscoe, G. L., and D. Summers (1981), Centrifugally driven diffusion of Iogenic plasma, *J. Geophys. Res.*, *86*(A10), 8471–8479, doi:10.1029/JA086iA10p08471.

Wilson, R. J., R. L. Tokar, M. G. Henderson, M. F. Thomsen, D. H. Pontius, and T. W. Hill (2007), Thermal plasma flow in Saturn's inner magnetosphere, *Eos Trans. AGU*, *88*(52), Fall Meet. Suppl., Abstract P43A–1020.

Wu, H., T. W. Hill, R. A. Wolf, and R. W. Spiro (2007a), Numerical simulation of fine structure in the Io plasma torus produced by the centrifugal interchange instability, *J. Geophys. Res.*, *112*, A02206, doi:10.1029/2006JA012032.

Wu, H., T. W. Hill, R. A. Wolf, and R. W. Spiro (2007b), Numerical simulation of Coriolis effects on the interchange instability in Saturn's magnetosphere, *Eos Trans. AGU*, *88*(52), Fall Meet. Suppl., Abstract P43A–1006.

Yang, Y. S., R. A. Wolf, R. W. Spiro, T. W. Hill, and A. J. Dessler (1994), Numerical simulations of torus-driven plasma transport in the Jovian magnetosphere, *J. Geophys. Res.*, *99*, 8755–8770, doi:10.1029/94JA00142.

Young, D. T., et al. (2005), Composition and dynamics of plasma in Saturn's magnetosphere, *Science*, *307*, 1262–1266, doi:10.1126/science.1106151.

Y. Chen and T. W. Hill, Department of Physics and Astronomy, Rice University, Houston, TX 77005, USA. (yichen@rice.edu)